Author/s:
Sant, S;Jenkins, MR;Dash, P;Watson, KA;Wang, Z;Pizzolla, A;Koutsakos, M;Nguyen, THO;Lappas, M;Crowe, J;Loudovaris, T;Mannering, SI;Westall, GP;Kotsimbos, TC;Cheng, AC;Wakim, L;Doherty, PC;Thomas, PG;Loh, L;Kedzierska, K

Title:
Human γδ T-cell receptor repertoire is shaped by influenza viruses, age and tissue compartmentalisation

Date:
2019-01-01

Citation:
Sant, S., Jenkins, M. R., Dash, P., Watson, K. A., Wang, Z., Pizzolla, A., Koutsakos, M., Nguyen, T. H. O., Lappas, M., Crowe, J., Loudovaris, T., Mannering, S. I., Westall, G. P., Kotsimbos, T. C., Cheng, A. C., Wakim, L., Doherty, P. C., Thomas, P. G., Loh, L. & Kedzierska, K. (2019). Human γδ T-cell receptor repertoire is shaped by influenza viruses, age and tissue compartmentalisation. Clinical and Translational Immunology, 8 (9), https://doi.org/10.1002/cti2.1079.

Persistent Link:
https://hdl.handle.net/11343/246770

Clinical & Translational Immunology

Australian and New Zealand Society for Immunology Inc.

Clinical & Translational Immunology 2019; e1079. doi: 10.1002/cti2.1079
www.wileyonlinelibrary.com/journal/cti

ORIGINAL ARTICLE

Human γδ T-cell receptor repertoire is shaped by influenza viruses, age and tissue compartmentalisation

Sneha Sant[1], Misty R Jenkins[2,3,4], Pradyot Dash[5], Katherine A Watson[2], Zhongfang Wang[1], Angela Pizzolla[1], Marios Koutsakos[1], Thi HO Nguyen[1], Martha Lappas[6], Jane Crowe[7], Tom Loudovaris[8], Stuart I Mannering[8], Glen P Westall[9], Tom C Kotsimbos[10,11], Allen C Cheng[12,13], Linda Wakim[1], Peter C Doherty[1,2], Paul G Thomas[5], Liyen Loh[1,a] & Katherine Kedzierska[1,a]

[1]Department of Microbiology and Immunology, University of Melbourne, at The Peter Doherty Institute for Infection and Immunity, Melbourne, VIC, Australia
[2]Immunology Division, Walter and Eliza Hall Institute, Melbourne, VIC, Australia
[3]LaTrobe Institute for Molecular Science, La Trobe University, Melbourne, VIC, Australia
[4]Department of Medical Biology, The University of Melbourne, Melbourne, VIC, Australia
[5]Department of Immunology, St Jude Children's Research Hospital, Memphis, TN, USA
[6]Obstetrics, Nutrition and Endocrinology Group, Department of Obstetrics & Gynaecology, Mercy Hospital for Women, University of Melbourne, Melbourne, VIC, Australia
[7]Deepdene Surgery, Deepdene, VIC, Australia
[8]Immunology and Diabetes Unit, St Vincent's Institute of Medical Research, Fitzroy, VIC, Australia
[9]Lung Transplant Unit, Alfred Hospital, Melbourne, VIC, Australia
[10]Department of Allergy, Immunology and Respiratory Medicine, The Alfred Hospital, Melbourne, VIC, Australia
[11]Department of Medicine, Central Clinical School, The Alfred Hospital Melbourne, Monash University, Melbourne, VIC, Australia
[12]School of Public Health and Preventive Medicine, Monash University, Melbourne, VIC, Australia
[13]Infection Prevention and Healthcare Epidemiology Unit, Alfred Health, Melbourne, VIC, Australia

Correspondence
L Loh or K Kedzierska, Department of Microbiology and Immunology, University of Melbourne, The Peter Doherty Institute for Infection and Immunity, Parkville, 792 Elizabeth St, Melbourne, VIC 3000, Australia.
E-mails: lohl@unimelb.edu.au or kkedz@unimelb.edu.au

[a]These authors contributed equally to this study.

Received 1 July 2019;
Revised 16 August 2019;
Accepted 17 August 2019

doi: 10.1002/cti2.1079

Clinical & Translational Immunology 2019; **8**: e1079

Abstract

Background. Although γδ T cells comprise up to 10% of human peripheral blood T cells, questions remain regarding their role in disease states and T-cell receptor (TCR) clonal expansions. We dissected anti-viral functions of human γδ T cells towards influenza viruses and defined influenza-reactive γδ TCRs in the context of γδ-TCRs across the human lifespan. **Methods.** We performed ^{51}Cr-killing assay and single-cell time-lapse live video microscopy to define mechanisms underlying γδ T-cell-mediated killing of influenza-infected targets. We assessed cytotoxic profiles of γδ T cells in influenza-infected patients and IFN-γ production towards influenza-infected lung epithelial cells. Using single-cell RT-PCR, we characterised paired TCRγδ clonotypes for influenza-reactive γδ T cells in comparison with TCRs from healthy neonates, adults, elderly donors and tissues. **Results.** We provide the first visual evidence of γδ T-cell-mediated killing of influenza-infected targets and show distinct features to those reported for CD8$^+$ T cells. γδ T cells displayed polycytotoxic profiles in influenza-infected patients and produced IFN-γ towards influenza-infected cells. These IFN-γ-producing γδ T cells were skewed towards the γ9δ2 TCRs, particularly expressing the public GV9-TCRγ, capable of pairing with numerous TCR-δ chains, suggesting their significant role in γδ T-cell immunity. Neonatal γδ T cells displayed extensive non-

overlapping TCRγδ repertoires, while adults had enriched γ9δ2-pairings with diverse CDR3γδ regions. Conversely, the elderly showed distinct γδ-pairings characterised by large clonal expansions, a profile also prominent in adult tissues. **Conclusion.** Human TCRγδ repertoire is shaped by age, tissue compartmentalisation and the individual's history of infection, suggesting that these somewhat enigmatic γδ T cells indeed respond to antigen challenge.

Keywords: human tissues, human γδ T cells, influenza virus infection, paired TCRγδ repertoire, public GV9-TCRγ clonotype

INTRODUCTION

Suggestive evidence indicates that γδ T cells are involved in diverse aspects of the host response, including acute and/or chronic inflammation, effective wound healing and the killing of virus-infected, cancerous and stressed cells.[1–4] In humans, γδ T cells respond to chronic viral infections, as suggested by their robust proliferative capacity during EBV reactivation,[5] the upregulation of effector functions during HIV persistence,[6] increased CD69 expression and expansion of δ1/δ3 T cells in kidney transplant patients with associated CMV latency.[7] In addition, phosphoantigen-expanded human γδ T cells upregulated IFN-γ and γδ T cells killed cells infected with human H1N1 and H5N1 influenza viruses.[8–11] Whether pre-activation is a requirement for killing of influenza virus-infected cells is unknown.

The way in which human γδ T populations change in diversity and prevalence with age for clinically normal, or currently challenged (by infection, cancer), individuals is far from clear. This provides a scope for analysis of clonal T-cell receptor (TCR) profiles within γδ T populations. In fact, rigorous TCR analysis currently provides our most accessible 'window' for dissecting γδ T-cell responses, as our present (and very limited) understanding suggests that the γδ TCRs bind antigens that are not presented by classical MHC-I molecules.[12] The dissection of clonality via TCR analysis has, until recently,[13,14] been limited by our inability to detect paired TCRγδ chains directly *ex vivo* for single cells. To date, paired analyses have demonstrated signatures of innate- and adaptive-like T cells in the $V\delta2^+$ $V\gamma9^+$ and $V\delta2^+$ $V\gamma9^-$, respectively, in human peripheral and umbilical cord blood (CB).[14,15] Analysis of TCR repertoire in chronic viral infections within patients suffering CMV reactivation following transplantation has been performed.[14,16] Antigen specificity and clonal expansions from both bulk analyses of $\gamma9^+$ or $\gamma9^-$ T cells,[14,16] and from paired analyses at the single-cell level, were observed,[15] suggesting that there may be specificity for the virus. It is unknown whether signatures of antigen specificity are apparent in other viral infections, particularly acute infections such as influenza virus. Moreover, how TCRγδ repertoires in healthy elderly adults evolve is unexplored, and there are limited data available on TCRγδ repertoires for lymphocytes recovered from human lymphoid and peripheral tissues.

Here, we utilise a novel multiplex single-cell RT-PCR[13] strategy to characterise paired TCRγδ clonotypes for T cells recovered directly from healthy neonates, adults and elderly donors. Different tissues were sampled, and the clonotypic analysis was also extended to T cells stimulated *in vitro* with influenza A viruses. Although (as compared to TCRαβ sets) γδ T cells display more limited TCR repertoires, our data demonstrate a diversity of TCRγδ pairings in CB (across different γδ segments and within γδ segments), in adults (diverse γδ TCRs within the predominant γ9δ2 segment but limited γδ segment usage), and in tissues (diverse distribution across γδ segments, plus clonal expansions within the segments). Additionally, older adults show individually skewed TCRγδ profiles, characterised by the predominant selection of largely expanded TCRγδ clones within selected γδ segments. In response to influenza-infected targets, γδ T cells elicit effective anti-viral functions such as killing and IFN-γ production. These influenza-specific IFN-γ-producing γδ T cells display the enrichment of γ9δ2 sets and the selection of public TCRγδ clonotypes across different donors. Our study is thus the first to analyse γδ TCR clonotype diversity

from subjects ranging in age from the neonates to the elderly. It seems that that TCRγδ repertoires vary with age, tissue compartmentalisation and prior infection suggesting that, as with the TCRαβ subsets, the varied prominence of particular clonotypes is shaped by an individual's history of antigenic exposure.

RESULTS

Kinetics of γδ T-cell-mediated killing of influenza virus-infected monocytes

As the efficacy of human γδ T cells to kill influenza-infected targets is far from clear, we assessed the mechanism of γδ T-cell-mediated killing using both the classic ^{51}Cr-release killing assay (Figure 1a, b) and a single-cell assessment using time-lapse live video microscopy[17–19] (Figure 1c, d, Supplementary figure 1). Our data clearly demonstrated that human γδ T cells obtained from adult donors could efficiently kill influenza H1N1/PR8-infected THP-1 monocytic targets directly *ex vivo*, as compared to uninfected controls (Figure 1a, b). Our subsequent in-depth assessment of the mechanism of γδ T-cell-mediated killing of PR8-infected THP-1 cells at 40× magnification revealed that γδ T cells were capable of recognising target antigen, as demonstrated by increase in intracellular Ca^{2+} concentration (as determined by Fluo-4 intensity; Figure 1c) in an average of 105 s after cell contact (Figure 1d, $n = 78$). Overall, the γδ T cells demonstrated an average of two Ca^{2+} fluxes, while in synapse with each target cell (Mean 2.04, $n = 96$; Figure 1e). We report for the first time that γδ T cells were capable of synapse formation and delivery of perforin to the virally infected target cells and target cell membrane blebbing occurred, indicative of morphologically distinct apoptotic target cell death (Figure 1c). In previous studies, uptake of PI through perforin pores into the cytosol has been used as a marker of perforin delivery to the target cells.[19] Here, we report that the time from antigen recognition, as denoted by the first Ca^{2+} flux in the γδ T cells, to the time of PI blush entering the target cell cytosol was an average of 276 s (4.6 min, $n = 7$; Figure 1). This time to degranulate is slower than has been previously reported for human $CD8^+$ T cells and NK cell of ~100 s.[18] Once the T cell has killed, it detaches from the dying target, and a high concentration of PI could be seen entering the target cell as it enters secondary necrosis (Figure 1c). The average time between the first T-cell Ca^{2+} flux to influenza-infected target cell blebbing (Figure 1f) and Ca^{2+} flux to T-cell detachment (known as synapse dwell time; Figure 1g) was comparable at 1000 s (mean = 1011 s, $n = 31$ and mean = 953 s, $n = 22$, respectively), across three independent human donors.

As shown in the representative montage of live cell imaging (Figure 1c) and the corresponding video (Supplementary figure 1), the kinetics of γδ T-cell-mediated killing only slightly vary to those previously reported in studies of human $CD8^+$ T-cell and NK-cell killing where a single Ca^{2+} flux was shown to be sufficient to trigger degranulation.[18] So while the γδ T cells do take longer to degranulate than $CD8^+$ T cells, the synapse dwell time of 16.4 min is consistent with previous reports on the kinetics previously shown in human $CD8^+$ T cells (~14 min) and human NK cells (~18 min)[17] (Figure 1g).

Taken together, we provide the first visual evidence of the mechanism underlying γδ T-cell-mediated killing of influenza-infected monocytic targets.

Vδ2$^+$ T cells display broadly cytolytic profiles in influenza virus-infected donors *ex vivo*

To further dissect the killing capacity of human γδ T cells directly *ex vivo*, we examined co-expression of cytolytic molecules Gzm A, B, K, M and perforin in patients naturally infected with influenza B viruses (IBV). An initial analysis of Gzm and perforin expression within the total γδ T-cell pool demonstrated high levels of Gzm A, M and perforin, with Gzm K being significantly lower in both healthy and IBV-infected adults (Figure 2; healthy adults, $P < 0.001$ Gzm A, M and perforin, $P < 0.01$ Gzm B; IBV-infected patients $P < 0.05$ Gzm A, M and perforin). In contrast, γδ T cells within the CB lacked Gzm A, B and K expression, with only Gzm M being moderately expressed (~15%, $n = 3$; Figure 2a). As Vδ2$^+$ and Vδ2$^-$ TCRγδ$^+$ subsets have previously shown to have differential functional capacities and phenotypic profiles,[20] we further segregated Gzm and perforin staining into Vδ2$^+$ and Vδ2$^-$ TCRγδ$^+$ subsets. Indeed, our frequency analyses of individual single cytotoxic molecules in healthy adults verified the previous findings and showed that the Vδ2$^+$ T cells had significantly higher

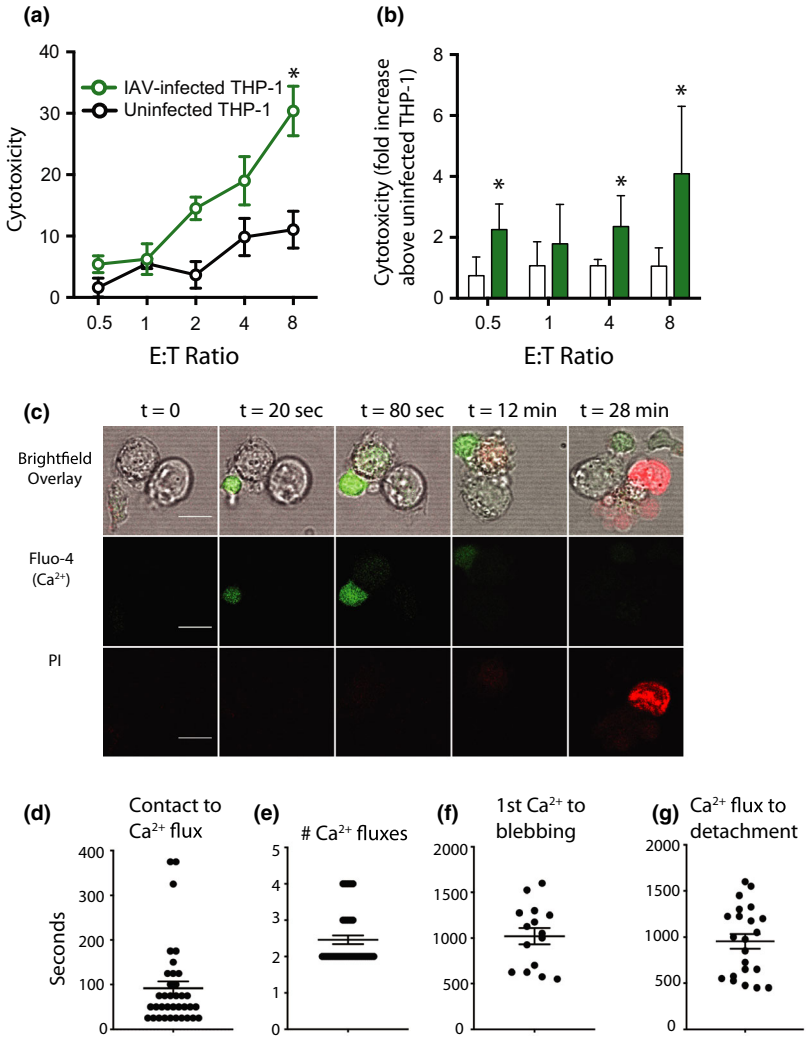

Figure 1. Human γδ T cells kill influenza virus-infected monocytic cells via apoptosis. **(a)** *Ex vivo* killing capacity of sort-purified, human γδ T cells assayed at multiple E:T ratios in a ^{51}Cr-release assay using influenza A virus-infected THP-1 cells (MOI 5). Representative plot from one donor assayed in triplicate, where the green line indicates γδ T cells incubated with IAV-infected THP-1 and the black line corresponds to uninfected THP-1 cells. The SEM is shown, $P = 0.001$, two-tailed *t*-test. Data are representative of three experiments. **(b)** The fold-change of specific lysis over uninfected THP-1. Pooled data from three donors assayed in triplicate, (mean ± SD, $P < 0.001$ (0.5:1), $P = 0.002$ (4:1), $P = 0.001$ (8:1), multiple *t*-tests. **(c)** Time-lapse microscopy of fluo-4-AM labelled γδ T cells killing IAV-infected THP-1 targets in the presence of 100 μM PI. Images were acquired every 10 s and show fluo-4(green)/PI(red)/brightfield overlay, with the single red and green channels in panels 2 and 3. Image is representative of 78 conjugates filmed. Scale bar = 10 μM. Quantitation includes the following: **(d)** the time from first membrane contact to calcium flux, **(e)** the overall number of Ca^{2+} fluxes, **(f)** the time from 1st Ca^{2+} flux to target membrane blebbing and **(g)** the time from 1st Ca^{2+} flux to T-cell detachment from the target cell. Panels **(d–g)** show mean ± SEM of pooled individual data from three human donors across three experiments.

frequency of all molecules with the exception of Gzm B than Vδ2$^-$ TCRγδ$^+$ cells (Figure 2b; P = Gzm A, K, M = 0.008, perforin = 0.023). These data suggest that Vδ2$^+$ T cells are superior in terms of polycytotoxic capability.

We thus subsequently analysed co-expression of multiple cytolytic molecules Gzm A, B, K, M and perforin Vδ2$^+$ and Vδ2$^-$ TCRγδ$^+$ subsets for both healthy donors (n = 8) and individuals naturally infected with IBV (n = 4; Figure 2c–f). Strikingly, when we visualised the co-expression patterns across five cytotoxic molecules (polyfunctional potential of γδ T cells), Vδ2$^-$ TCRγδ$^+$ T cells in IBV-infected individuals had highly polycytotoxic profiles (Figure 2c) in comparison with healthy adult donors, which displayed a higher proportion of Vδ2$^-$ TCRγδ$^+$ T cells lacking Gzms and perforin (GzmA$^-$B$^-$K$^-$M$^-$Perf$^-$ cells; Figure 2e; P = 0.049).

However, the polyfunctional polycytotoxic profiles within Vδ2$^+$ T cells were comparable across IBV-infected and healthy donors (Figure 2d).

In summary, although Vδ2$^+$ T cells display a highly potent cytotoxic potential in healthy and IBV-infected donors, Vδ2$^-$ TCRγδ$^+$ T cells upregulate their cytotoxic profiles in IBV-infected in a way that the majority of cells express a combination of 4–5 cytotoxic molecules. The key question arises whether killing of influenza-infected targets is mediated via specific TCRγδ clonotypes or, alternatively, via all the available TCRγδ clonotypes.

Potent upregulation of IFN-γ by γδ T cells following exposure to influenza-infected targets

As it is technically difficult to sequence TCRs of γδ T cells killing influenza-infected targets, we further identified influenza-specific γδ T cells via IFN-γ production in an *in vitro* assay using influenza virus-infected lung epithelial cell line (A549) and peripheral blood mononuclear cell (PBMC) co-culture system (Figure 3a).[21] Infection of the A549 cells with influenza A (PR8-IAV) and B viruses for 10 h resulted in an infection rate of ~85% (Figure 3b; 78–90% $n = 5$), measured by intracellular staining with anti-influenza nucleoprotein. In healthy adults, we observed a significant upregulation of IFN-γ production by γδ T cells after co-culture of PBMCs with IAV-infected A549s, 15.7-fold above co-culture with uninfected A549 cells (mean 4.7%; Figure 3c, e, $P < 0.01$, $n = 16$). Furthermore, ~80% of IFN-γ-producing γδ T cells expressed Gzm B (Supplementary figure 2), suggesting that the majority of influenza-reactive γδ T cells have the potential to kill IAV-infected target cells. Minimal IFN-γ production towards IAV-infected A549 cells was detected in CB γδ T cells (Figure 3c, e). In contrast, CB-derived NK cells could respond to IAV-infected A549 cells by secreting IFN-γ (Figure 3d). These data suggest that in the context of IAV infection, neonatal γδ T cells have a naïve-like functional profile, which is supported phenotypically by their predominant lack of cytotoxic molecule expression *ex vivo* (Figure 2a). Co-culture of adult PBMCs with IBV (B/Massachusetts/02/2012)-infected A549s resulted in comparable upregulation of IFN-γ production towards IAV (Figure 3e) and IBV (Supplementary figure 3) infected by adult γδ T cells. Together, our data show that adult peripheral blood γδ T cells display potent heterosubtypic immunity against influenza A and B viruses.

To understand the mechanisms underlying the activation of γδ T cells during influenza virus infection, we assessed the role of soluble inflammatory mediators released during influenza virus infection of A549 cells on the activation of γδ T cells. Supernatants were collected from PBMCs co-cultured with IAV-infected A549 cells or uninfected controls. These supernatants were then transferred to autologous PBMCs, followed by the assessment of IFN-γ and TNF expression (Figure 3f). Autologous PBMC stimulated with supernatants from IAV-infected A549:PBMC co-cultures had significant reduction in IFN-γ production when compared to the original PBMCs co-cultured with IAV-infected A549s (Figure 3 g, h, $n = 6$, $P = 0.026$), indicating that inflammatory mediators alone are insufficient at inducing γδ T-cell activation. To dissect the requirement of a particular cell subset for mediating γδ T-cell activation, we depleted monocytes from our co-culture system, as monocytes were previously involved in γδ T-cell stimulation during dengue infections.[22] Depletion of CD14$^+$ monocytes from PBMCs co-cultured with IAV-infected A549s significantly diminished IFN-γ production ($P = 0.0026$; Figure 3i, j), suggesting that monocytes mediate, partially, γδ T-cell IFN-γ production towards IAV-infected lung epithelial cells.

Taken together, we demonstrate that γδ T cells can potently upregulate IFN-γ during heterosubtypic influenza infection and such activation depends, at least partially, on monocytes is not modulated by soluble mediators derived from *in vitro* IAV infection of lung epithelial cells.

γ9δ2 T cells are the major IFN-γ producers during influenza virus infection

To probe γδ TCRs activated following influenza virus infection, we paired an influenza virus-infected lung epithelial and PBMC co-culture system (Figure 3a)[21] with an IFN-γ cytokine capture assay to isolate influenza-reactive γδ T cells for paired single-cell TCR analyses[23] (Figure 4a, Supplementary figure 4).

Paired TCR γδ analyses from IFNγ$^+$ cells stimulated with IAV-infected A549 and PBMCs (Figure 4a, $n = 3$ adult donors) revealed that IFN-γ$^+$ γδ T cells consisted almost exclusively of γ9δ2 cells (90.3%; Figure 4b, d, Supplementary table 5). The majority of IFN-γ-negative TCRs were Vδ2 paired with a broad range of Vγ-chains (Vγ3,

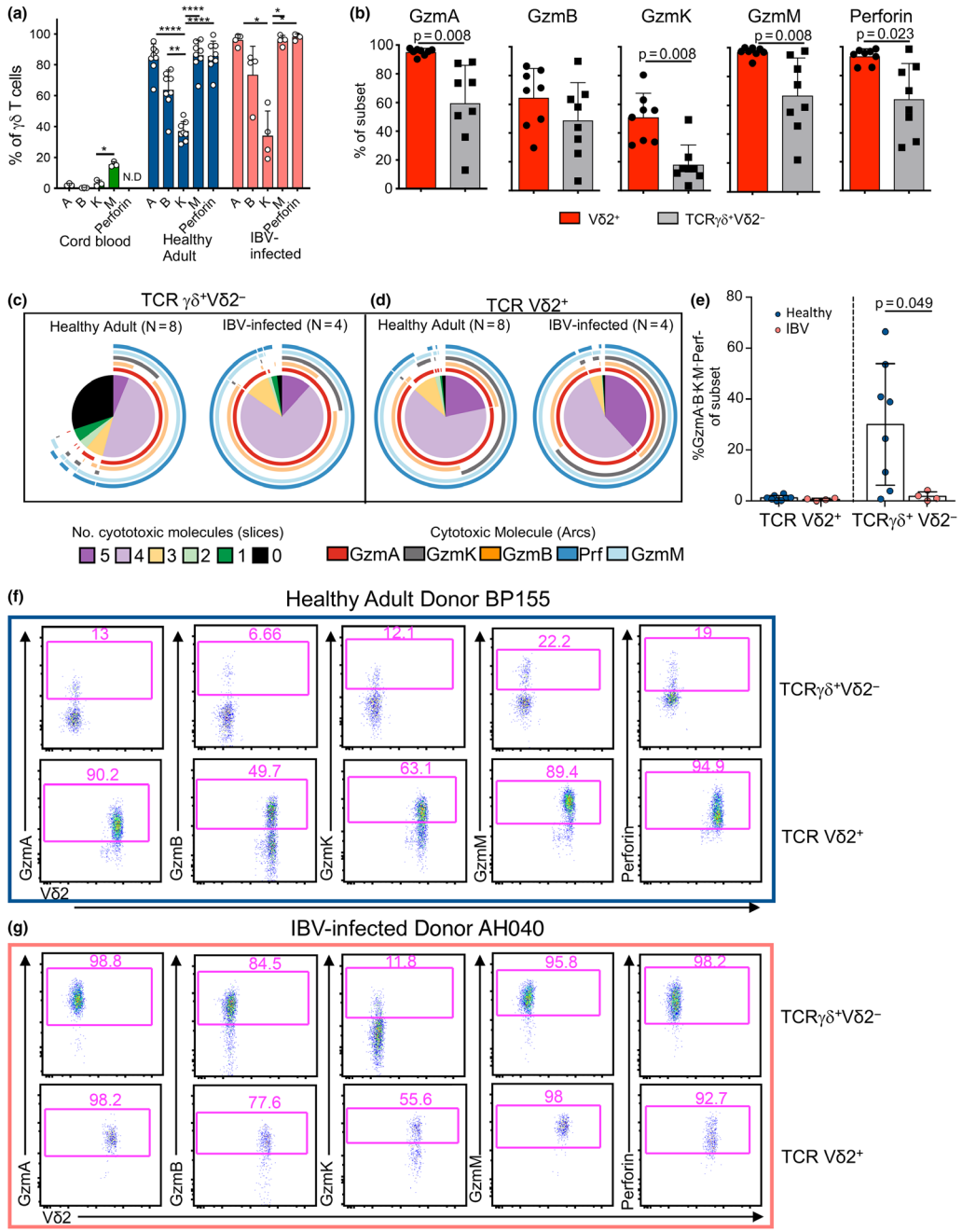

Figure 2. Vδ2$^+$ γδ T cells display broadly cytotoxic profiles which persist in influenza B virus-infected donors. TCRγδ$^+$CD3$^+$ T cells within the cord blood (CB; n = 3), peripheral blood in healthy adults (n = 8) or influenza B virus (IBV)-infected donors (n = 4, where one donor has two timepoints post-infection), were identified directly *ex vivo*. **(a)** Total granzymes and perforin expression in total γδ T cells from cord blood, healthy adult peripheral blood mononuclear cell (PBMC) and IBV-infected donors, ANOVA one-way. **(b)** Gzm A (p = 0.008), Gzm B, Gzm K (P = 0.008), Gzm M (P = 0.008) and perforin (P = 0.023) expression in Vδ2$^+$ (red) and Vd2$^-$ (grey) subsets from PBMC in healthy adults (n = 8), Wilcoxon test. (cd) Co-expression of cytotoxic molecules in **(c)** Vδ2$^-$ TCRγδ$^+$ and **(d)** Vδ2$^+$ T cells from healthy (n = 8) and IBV-infected (n = 4) adult donors is depicted in the pie charts. The segments correspond to the number of co-expressed cytotoxic molecules, and the cytotoxic molecule is specified by the arcs. Pie charts were generated with Pestle and SPICE software.[39] **(e)** Shown is the proportion of Vδ2$^+$ and Vδ2$^-$ TCRγδ$^+$ cells not expressing Gzms A, B, K, M and perforin in healthy (n = 8) and IBV-infected (n = 4) adult donors. P = 0.049, Mann–Whitney test. (**f, g**) Representative FACS plots of intracellular Gzm A, B, K, M and perforin staining in Vδ2$^+$ or Vδ2$^-$ TCRγδ$^+$ T cells from **(f)** healthy adult and **(g)** IBV-infected donor PBMC.

Vγ4, Vγ5, Vγ8, Vγ9 and Vγ10; Figure 4c, Supplementary table 5), suggesting that IFNγ$^+$ cells were indeed antigen-responsive. The majority of Vγ9Vδ2 TCRs had JP*01 at J-junctions, characteristic of the previously described phosphoantigen-reactive TCRs (Supplementary figure 5). Analyses of the CDR3δ region showed the conserved hydrophobic amino acid at position 97 (Supplementary table 5), as in phosphoantigen-reactive TCRs (L, V, I, A and M).[24] We speculate that in our system, IAV infection may upregulate phosphoantigen metabolites, given the similarities of the CDR3 region with phosphoantigen-reactive γδ TCRs.

Thus, the γδ TCR profiles for IFN-γ-producing T cells stimulated with IAV-infected lung epithelial cells were characterised by a bias in γ9δ2 TCR usage, and whether these TCRs are present across the human lifespan is unknown.

Differential TCR usage and pairing of γδ chains across the human lifespan

Although the Vδ2$^+$ T cells were predominately found in peripheral adult blood, we sought to understand whether γδ TCR repertoires across the human lifespan (though not within individuals) display signatures of antigen experience. Firstly, to understand how human γδ T cells change with age and tissue compartmentalisation, we dissected directly *ex vivo* CD3$^+$ TCRγδ$^+$ T cells within the PBMCs of 29 healthy adult (AD) donors (18–59 years, median 33 years), 28 healthy elderly (ED) donors (≥60 years, median 75.3 years) and 16 CB samples (Figure 5a, Supplementary table 1). While the frequency of γδ T cells was lower in CB (1.6% ± 0.9), it significantly increased in healthy adult PBMCs (4.0% ± 4.4, $P < 0.05$) and was variable (0.2–9.3%; mean of 3.7% ± 4.6) in healthy elderly individuals (Figure 5b). γδ T cells in human tissues [spleen (SP) and lymph nodes (LN)] showed a higher proportion in spleen (7.2% ± 1.27) and were of lower frequency in LN (0.5% ± 0.13), than those in adult peripheral blood (Figure 5b).

To define TCRs across the human lifespan, we used a recently established single-cell nested RT-PCR[13] for unbiased, paired *ex vivo* analysis of γ and δ CDR3 sequences recovered from healthy donor PBMCs [CB (n = 3), AD (n = 3), ED (n = 4)] and tissues [SP (n = 3), lung (LG; n = 3), LN (n = 2); Supplementary figure 4]. In all, we analysed 467 paired γδ TCR sequences, 309 from PBMCs and 158 from lymphoid and lung tissues (Supplementary tables 3 and 4). In umbilical CB, we observed diverse V-region usage for both the Vγ (Vγ2, Vγ3, Vγ4, Vγ5, Vγ8, Vγ9 and Vγ10) and Vδ (Vδ1, Vδ2, Vδ3, Vδ4 and Vδ5) segments (Figure 5c, Supplementary figure 3A, Supplementary table 3). Strikingly, neonatal repertoires were polyclonal with unique CDR3γδ sequences found across different donors (Figure 5c Supplementary figure 6a, Supplementary table 3). Overall, Vδ1 could pair with diverse Vγ segments (Vγ2–5, Vγ8 and Vγ10), while Vδ2 paired predominantly with Vγ9 (12–35%), and less commonly with Vγ3 (4–10%), Vγ4 in CB1, Vγ5 in CB2 and Vγ8 in CB3 (4%; Figure 5c). In contrast, the predominant TCR usage in adult γδ T cells was Vγ9 paired with Vδ2 (mean 70.3%; Figure 5d, Supplementary figure 6b, Supplementary table 3), albeit with a high diversity of unique Vγ and Vδ CDR3 sequences (mean of clonotypes was 53 out of 53 Vγ9Vδ2 sequences; Supplementary table 3).

The CD3/TCRγδ complex has been previously shown to segregate γδ T cells into two subsets, TCRγδ^{hi}/CD3^{lo} and TCRγδ^{lo}/CD3^{hi} in ratio, with distinct effector functions between the populations.[25,26] These phenotypes may reflect γδ T-cell clonal expansion driven via TCR-mediated interactions with antigen.[26] As we know so little about these responses, we were particularly interested in probing our data sets for this parameter. Co-staining for CD3 and TCRγδ identified both TCRγδ^{lo}/CD3^{hi} and TCRγδ^{hi}/CD3^{lo} populations in two out of four elderly individuals (ED1, ED14, Supplementary figure 8), while we did not observe segregated populations in the three CB and adult donors we analysed for TCR repertoires. Observed for ED1 and ED14, the majority of the γδ T population expressing TCRγδ^{lo}/CD3^{hi} cells had dominant Vδ1 usage (Figure 5e). This was converse to previous studies showing predominant Vδ2 usage in the TCRγδ^{lo}/CD3^{hi} subset,[26] suggesting that the TCRγ^{lo}/CD3^{hi} in the elderly may reflect recent TCR-dependent activation. The subset of γδ T cells expressing TCRγδ^{hi}/CD3^{lo} had the predominant usage of Vδ2 paired with Vγ2 (ED1, Figure 5e, Supplementary tables 3 and 4), where Vδ2 paired with Vγ9 or Vδ1 paired with Vγ4 (ED14, Figure 5e, Supplementary table 4, Supplementary figure 6c, Supplementary table 3). Furthermore, large clonal expansions were also observed in the both TCRγδ^{hi}/CD3^{lo} and TCRγδ^{lo}/CD3^{hi} subsets from the elderly. In ED1, both subsets had one repeated clone, each contributing 87% and 93% to the repertoire. ED14

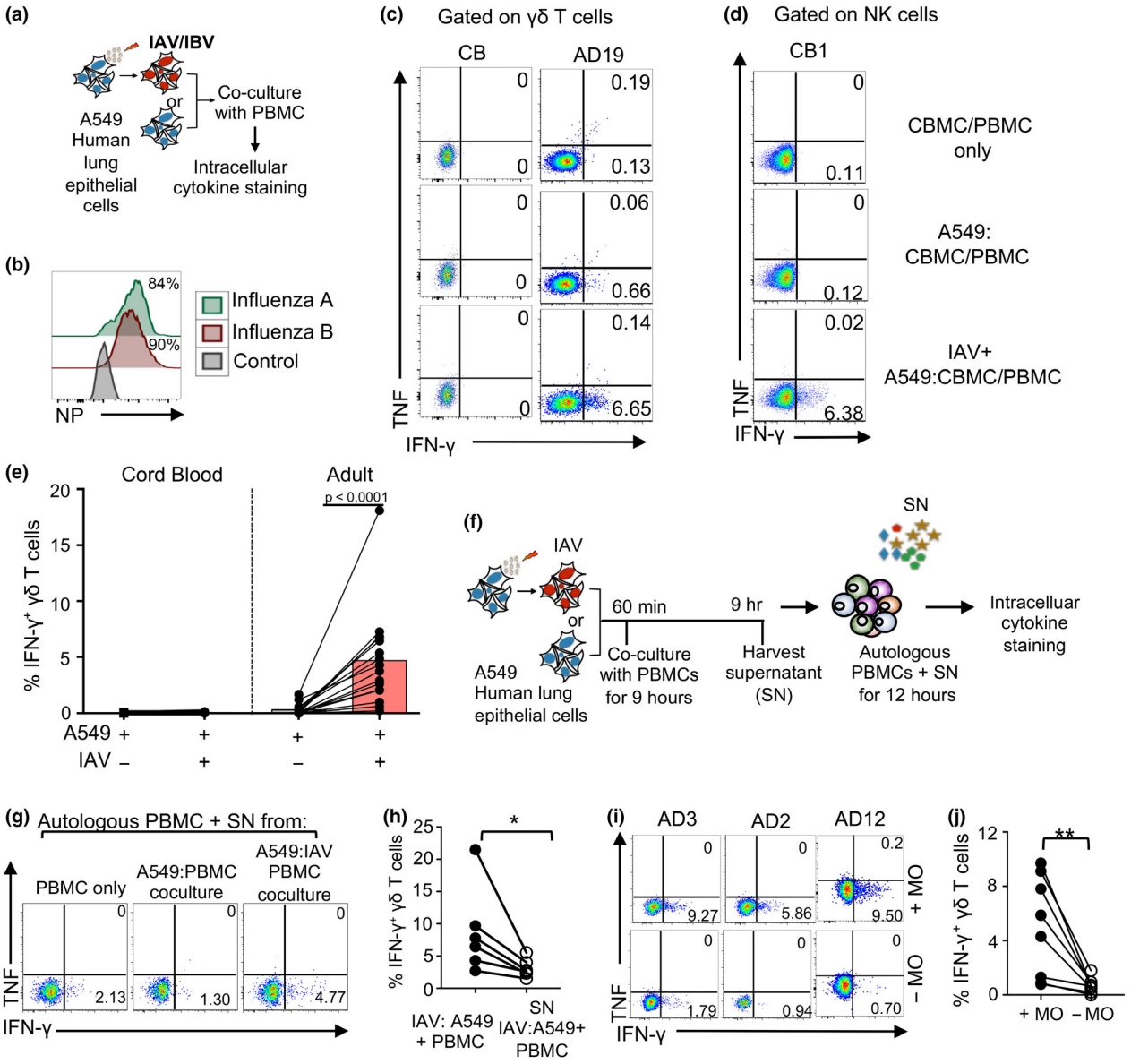

Figure 3. Influenza virus infection triggers IFN-γ upregulation in γδ T cells which requires soluble factors and monocytes. **(a)** Schematic representation of an *in vitro* influenza-infected human lung epithelial cell (A549):peripheral blood mononuclear cell (PBMC) co-culture assay.[21] A549 cells were infected with influenza A (IAV; A/Puerto Rico/8/1934 H1N1) or B (IBV; B/Massachusetts/02/2012) viruses (PR8, H1N1) for 1 h, washed and subsequently co-cultured with PBMCs for 9 h (in the presence of BFA for the last 6 h). Cytokines were measured via intracellular staining. **(b)** Influenza A virus and IBV nucleoprotein staining in A549 cells 10 h post-infection. **(c)** Representative FACS plots show IFN-γ production by γδ T cells in cord blood (CB) and adult peripheral blood for 'PBMC only' controls (top), uninfected A549 cells (middle) and IAV-infected A549 cells (bottom). **(d)** IFN-γ responses of cord blood NK cells ($CD56^+$ $CD3^-$) when CB lymphocytes were co-cultured with IAV-infected A549 cells, uninfected A549 control and PBMC only control. **(e)** The frequency of IFN-γ^+ producing γδ T cells in CB (n = 3) and adults is shown during IAV:A549 (n = 16 Adults) co-cultures. Background cytokine production by γδ T cells from PBMC only was subtracted from co-cultures of PBMC with uninfected/virus-infected A549 cells. Mann–Whitney test was performed between A549 uninfected and A549 IAV-infected adults (n = 16), P = < 0.0001. **(f)** Schematics of supernatant transfer experiments. A549 cells were infected with IAV for 1 h prior to co-culture with PBMCs for 9 h (in the absence of BFA). Supernatant (SN) from uninfected or IAV-infected co-cultures were used to stimulate autologous PBMCs to measure IFN-γ production and TNF upregulation. **(g)** Representative FACS plots show IFN-γ and TNF production in adult peripheral blood γδ T cells during SN transfer and summarised in **(h)** (n = 6). Wilcoxon test, *P < 0.05. **(i)** Representative FACS plots show IFN-γ and TNF production after monocyte depletion from PBMC in an *in vitro* influenza-infected A549 assay and summarised in **(j)** (n = 8). Wilcoxon test, **P < 0.01.

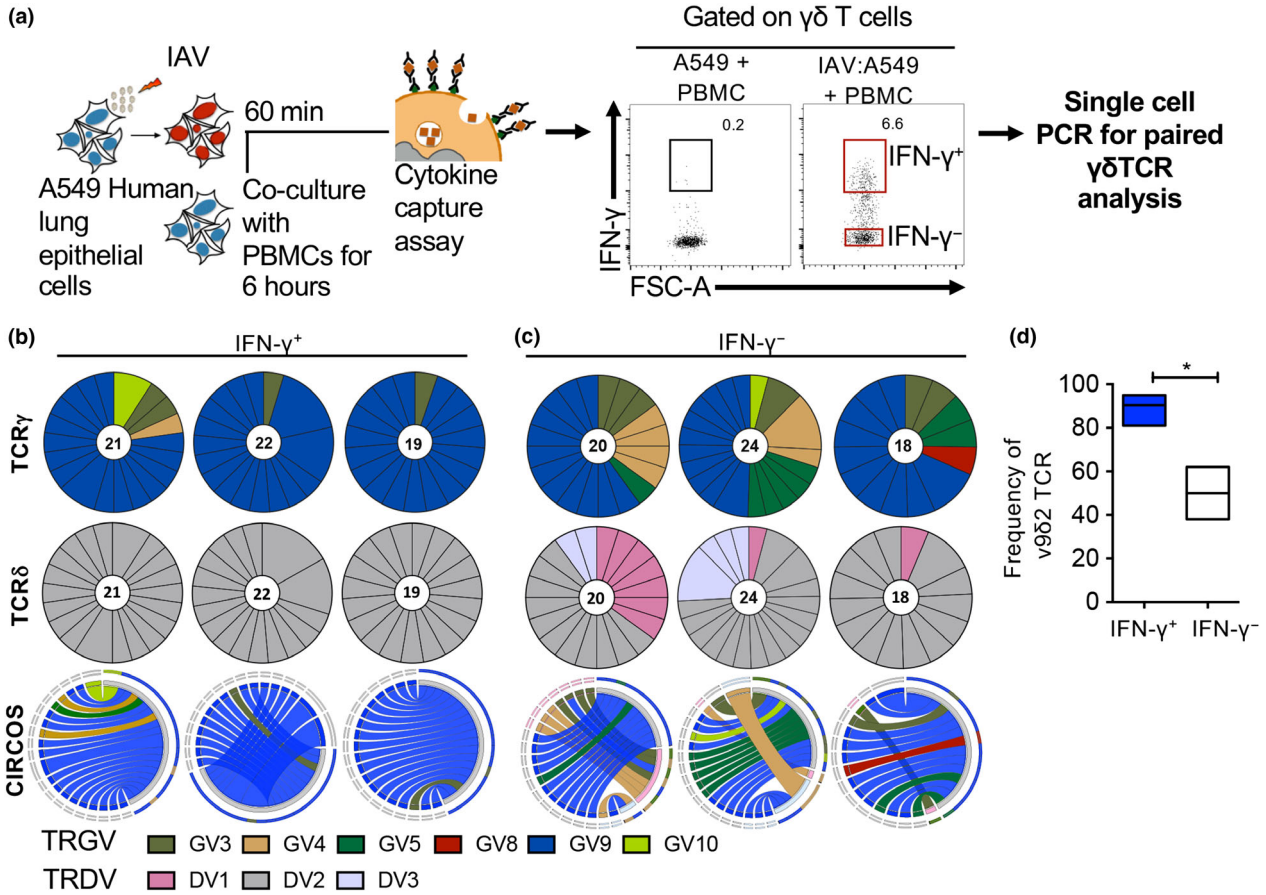

Figure 4. Dominance of the γ9δ2 T-cell subset within IFN-γ producers after *in vitro* influenza infection. **(a)** Schematic representation of IFN-γ secretion assay was performed after *in vitro* influenza A (IAV)-infected A549 cells were co-cultured with peripheral blood mononuclear cell for 6 h. For single-cell sorting and RT-PCR analysis, for paired γδ TCRs, IFN-γ secretion assay was used as a readout of influenza-reactive γδ T cells. (**b, c**) Vγ (top) and Vδ (bottom) usage in **(b)** IFN-γ$^+$ and **(c)** IFN-γ$^-$ γδ T cells is shown, with each segment representing a unique CDR3 region and each colour marking a specific subset of TRGV or TRDV gene usage. Circos plots (lower panel) of frequencies of Vγ-J and Vδ-J usage in paired TCR γδ sequences are shown for IFN-γ$^+$ and IFN-γ$^-$ γδ T cells. Each segment represents a unique clone, and segment thickness corresponds to frequency. **(d)** Frequency of γ9δ2 TCRs within IFN-γ$^+$ γδ T cells is higher than within IFN-γ$^-$ γδ T cells after IAV-A549 co-culture (Mann–Whitney test; *$P < 0.05$).

had two largely expanded clonotypes in the TCRγδ^{hi}/CD3^{lo} population and one large clonotype in TCRγδ^{lo}/CD3^{hi} subset, representing 32% and 72% of the total repertoire (Supplementary tables 3 and 4, Figure 5e, Supplementary figure 6c). In the remaining two elderly donors (ED4, 5), preferential Vγ9Vδ2 pairing and large clonal expansions of private γδ clonotypes were observed (Figure 5e, Supplementary table 4, Supplementary figure 6c, Supplementary table 3), suggesting narrowing of the TCR γδ repertoire. Together, these data suggest that large clonal expansions of particular γδ T-cell clonotypes with ageing and the TCRγδ^{lo}/CD3^{hi} γδ T-cell populations found in the elderly are most likely to reflect the expansion of a Vδ1 repertoire in response to *in vivo* stimuli.

We analysed the CDR3γδ length distribution at the amino acid (aa) level (Supplementary figure 69) to identify further signatures of antigen experience in the elderly as suggested by their expanded clonotypes. In contrast to neonates and adults with CDR3 length characterised by a normal distribution (Supplementary figure 9a, b), γδ T cells in the elderly showed profound perturbations and a non-normal distribution with the CDR3δ length ranging from 11 to 28 aa and CDR3γ length ranging from 9 to 17 aa (Supplementary figure 9c), coinciding with accumulation of clonal expansions of γδ T cells during ageing, as found for TCRαβ clonotypes.[27,28]

Thus, paired γδ TCR analyses indicate that the alterations in TCR γδ segment usage and γδ

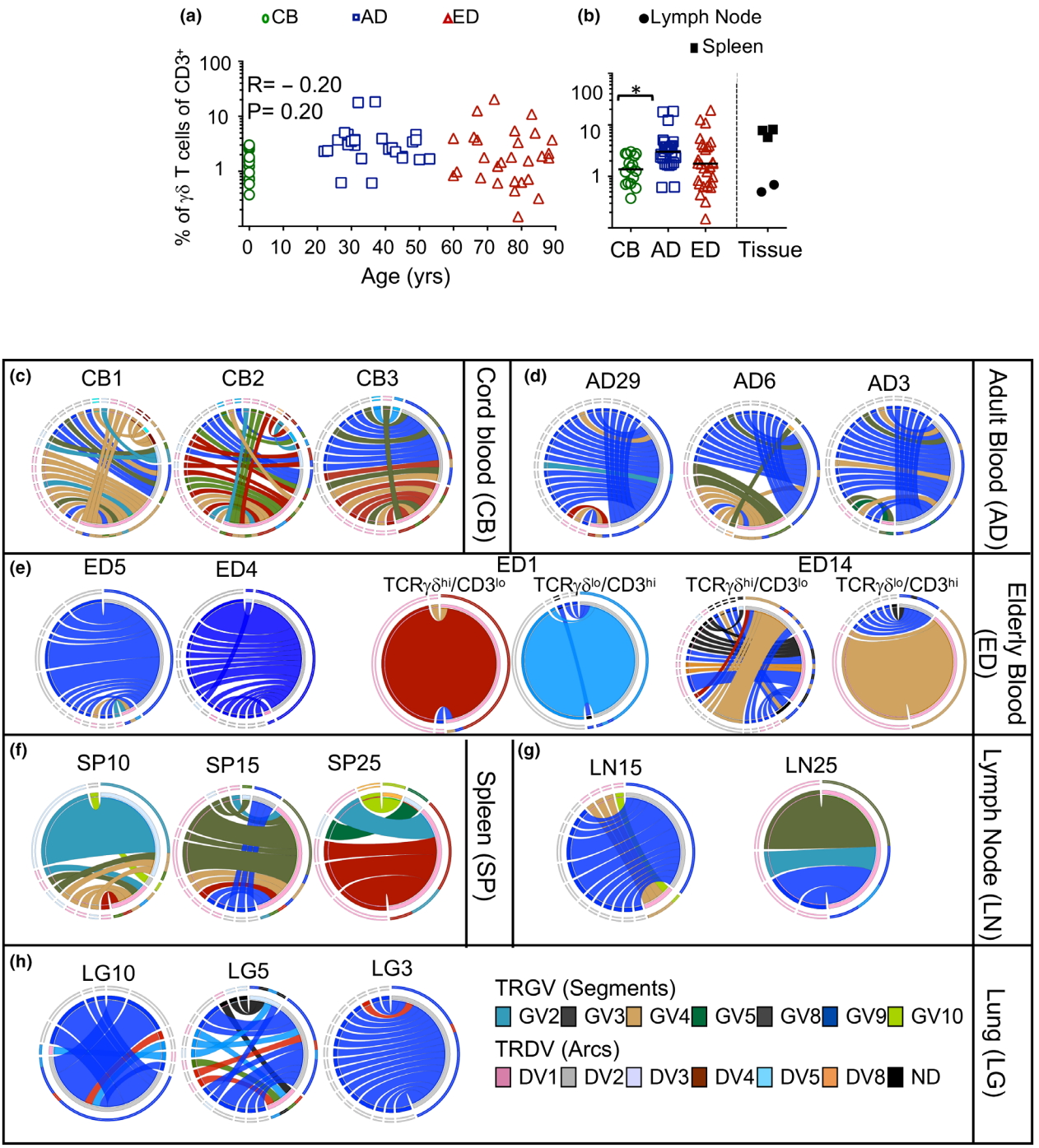

Figure 5. CDR3γδ composition and diversity are shaped by age and tissue localisation (**a, b**) The frequency and CD3 expression of human γδ T cells differs with age. TCRγδ^{+}CD3^{+} T cells within the cord blood (CB; n = 16) or peripheral blood in adults (AD; n = 26) or elderly donors (ED; n = 24) and tissues (SP and LN) were identified directly *ex vivo*. T-cell frequencies in **(a)** representative donors or **(b)** across individual cord blood, adult and elderly adult donors are shown. The correlation between the % frequency of γδ^{+}CD3^{+} T cell and age was assessed using the Spearman rank test. **(c–h)** Circos plots of frequencies of Vγ-J and Vδ-J usage in paired TCRγδ sequences are shown for **(c)** CB, **(d)** AD, **(e)** ED, **(f)** SP, **(g)** LN (n = 2) and **(h)** LG (n = 3 each, respectively, unless specified). **(e)** In selected donors, γδ TCR clonotypes were dissected based on the ratio of γδTCR and the CD3 complex, γδTCR^{lo}/CD3 and γδ TCR^{hi}/CD3 populations.[40] Each segment represents a unique clone, the segment colour corresponds to the TRGV gene usage, and the thickness corresponds to frequency. The coloured arcs represent the TRDV usage. Circos plots were generated with the circos software package.[41] Annotated Circos plots are shown in Supplementary figure 7.

pairing occur during human lifespan may underlie differential functional potential and/or antigen experience for human γδ T cells.

Diverse γδ segment usage and large clonal expansions in human lymphoid and peripheral tissue TCRs

As the TCRγδ repertoire can be thought to be dictated by antigen recognition at different anatomical sites and the paired TCRγδ composition in human lymphoid and peripheral tissues is unknown, we performed *ex vivo* analysis of paired TCRγδ repertoire in human SP, LN and LG. Spleen25 and LN25 were derived from BD25 donor with confirmed influenza disease, and SP15 and LN15 were obtained from the clinically normal BD15 donor. In two donors, the dominant Vδ1 was observed in spleen and in the LN of LN25 (Figure 5f, g). Paired TCRγδ analyses in SPs ($n = 3$) and LNs ($n = 2$) showed intra-donor variations in both variable gene usages, with the dominant γδ pairing being γ2δ3 (SP10), γ8δ1 (SP15) and γ3δ1 (SP25) for spleen, γ9δ2 (LN15) and γ5δ1 (LN25) for LN s, and γ9δ2 for all lungs, respectively (Figure 5f, h). A single clone was found to be shared between the LN and SP in influenza-infected donor BD25 (Supplementary table 5), and this was not evident in the clinically normal donor BD15 with paired LN and SP analyses. It is thus tempting to speculate that this TCRγδ clone might be influenza-specific. Interestingly, in the lung tissue recovered from all three donors, the TCRγδ repertoires were dominated by γ9δ2 clones across all LG donors.

Akin to elderly donor TCRγδ repertories, large clonal expansions were observed in 2 LN donors (LN25, LN15 at 70% and 34% of repertoire), three spleen donors (SP10, SP15 and SP25 at 22%, 57% and 94% of repertoire) and three lung donors (LG10, LG3 and LG5 at 68%, 20% and 22% of repertoire; Supplementary table 4). Strikingly, in these donors, cumulative analyses of TCRγδ CDR3s in the respective tissues also demonstrated a non-normal distribution, with the dominant CDR3 lengths within individuals being: 9 aa and 17 aa (SP), 7 aa and 18 aa (LN), and 12 aa and 17 aa (LG) for γ and δ TCR chains (Supplementary figure 9d–f). This suggests that skewing of CDR3γδ profiles in lymphoid and lung tissues is most likely to reflect the presence of substantially expanded clonotypes, the profile found consistently for the elderly γδ TCRs in peripheral blood.

Together, our analyses of TCRγδ repertoire and CDR3γδ distribution indicate that γδ T cells exhibit a compartmentalised structure dependent on age and anatomical location.

Shared features of healthy and influenza virus-reactive γδ T cells and analysis of the public CDR3γδ sequences across different ages and tissue compartments

With a total of 467 TCRγ sequences across different age groups and lymphoid and lung tissues, we analysed shared features within the CDR3γδ repertoires. We first probed our blood data set for the canonical Vγ9 public CDR3γ-CALWEVQELGKKIKVF,[29] which was found in all the adult donors (at 8–16%) as well as CB2 (at 4%), ED4 (at 4%), and in the TCRγδ^{lo}/CD3^{hi} subset of ED14 (at 12%; Supplementary table 7). Our pairing analysis for the TCRγδ chains shows the public CDR3γ-CALWEVQELGKKIKVF TCR has the capacity to pair with 13 different CDR3γ-DV2 chains in blood, across age groups (Figure 6a, Supplementary table 8). Strikingly, all donors with influenza A virus-responsive γδ T cells (Figure 4b) showed the presence of public CDR3γ9–CALWEVQELGKKIKVF sequences (at 10%, 24%, 10%) in IFN-γ$^+$ γ9δ2 segments (Supplementary table 5). Furthermore, as in the adult blood, the canonical Vγ9 public was found in LG5 and LG10 (Figure 5h, Supplementary table 7). The prominence of public clones in 2/3 lung tissues (Figure 6b, pink segments) analysed for TCRγδ repertoire suggested its importance in human immune responses, where these clonotypes have the potential to contribute to antigen-driven responses in peripheral tissue.

Aiming to define possible governing motifs for CDR3γδ TCR recognition, and to determine whether IAV-reactive γ9δ2$^+$ cells had unique CDR3 γδ motifs, we performed an in-depth analysis of amino acid usage at the CDR3γ and CDR3δ regions with common found aa lengths between healthy adult TCR γδ and IFN-γ$^+$ γ9δ2 TCRs. We used Seq2logo to generate aa sequence motifs which would allow us to identify potential differences between the CDR3γ and CDR3δ regions between healthy adult TCR γδ and influenza-responsive IFN-γ$^+$-γ9δ2 TCRs. Surprisingly, the pattern of aa usage presented no differences in the motifs between these two groups, thus indicating that healthy adult

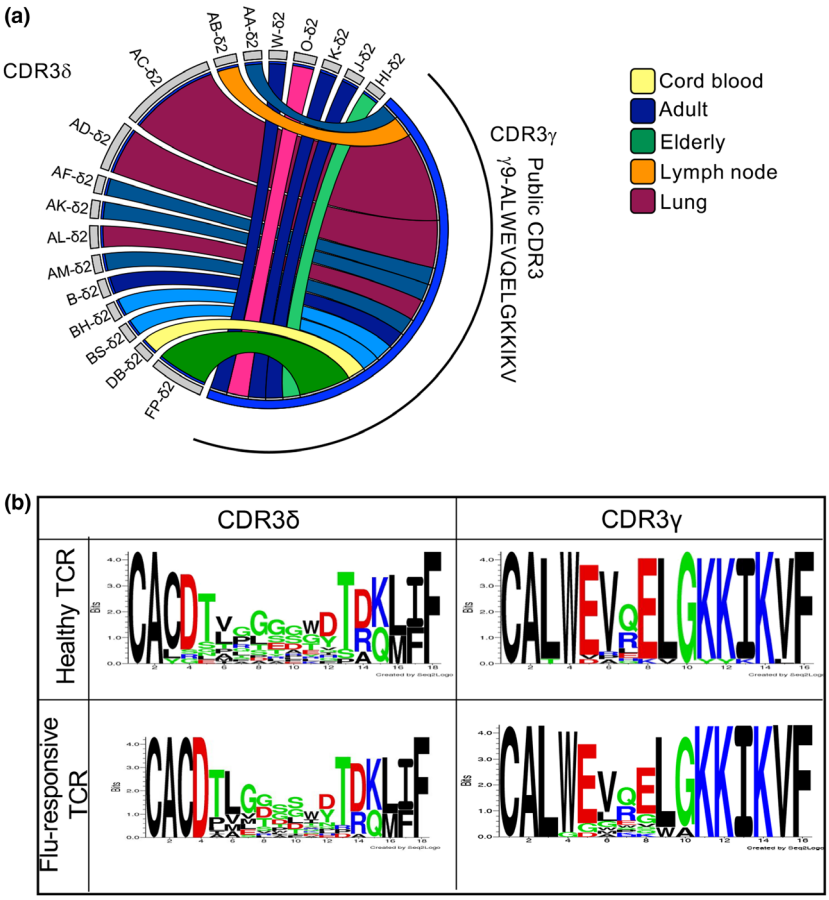

Figure 6. Public CDR3γδ sequences across different ages and tissue compartments. **(a)** A circos plot showing pairings of the public γ9-CALWEVQELGKKIKVF with diverse δ2-chains is shown for different age groups (cord-yellow, adult-blue, elderly-green) in blood, lymphoid (orange) and lung tissues (pink), and donors are represented by shades of each distinct colour. The thickness of each segment correlates to the size of the clone. Codes of donors utilising public γ9-chain pairings are specified in Supplementary table 7. **(b)** Amino acid enrichments within CDR3γ and CDR3δ regions of the most prevalent CDR3 length in healthy donors [14 amino acid (a.a.)] compared to the IFN-γ^+ γδ TCRs (14a.a.). Graphics were generated using Seq2Logo (Denmark).

peripheral blood γδ T cells are enriched with influenza-reactive γδ T cells (Figure 6b).

Our data suggest that the majority of healthy adults are circulating γδ T cells that have the potential to mediate anti-viral immunity against IAV infection, whereas lack of γ9δ2 TCRs in some elderly donors and CB γδ T cells could signify vulnerability to such viruses. Moreover, the presence of public γ9 TCRs in lung tissues further supports their role in mediating anti-influenza immunity.

DISCUSSION

Given the immunomodulatory potential of γδ T cells and the recent evidence on the importance of γδ T cells and their specific TCRs in bacterial, viral infections and cancer,[3,16,30,31] we dissected the anti-viral potential of human γδ T cells towards influenza-infected cells. We provide the first visual evidence of γδ T cells killing influenza-infected targets and show very similar features of γδ T-cell-mediated killing to those previously reported for human $CD8^+$ T cells.[17,18] The synapse dwell time of T cells with their targets is indicative of the efficiency of cytotoxicity, and we report here for the first time that γδ T cells are capable of forming a functional immune synapse and inducing apoptosis of infected target cells with an equivalent efficiency to $CD8^+$ T cells and NK cells. It is also worth noting that we did not see any PI uptake into the γδ T effector T cells themselves, indicating that perforin delivery was unidirectional and that γδ T cells did not undergo any cell death themselves as a result of cytotoxicity of targets.

Interestingly, the rate of degranulation was slower than has been observed in $CD8^+$ T cells, potentially highlighting differences in signalling thresholds to induce cytotoxicity. In previous studies, granule recruitment in both $CD4^+$ T cells, and in $CD8^+$ T cells with CD8 blockade, has been shown to release cytotoxic granules more slowly than $CD8^+$ T cells,[32] shown to be due to weaker recruitment of the microtubule-organising centre to the synaptic membrane. In a similar study, altered peptide ligands were used in a $CD8^+$ T-cell system to show that peptide interaction strength can determine the early signalling kinetics for degranulation and cytotoxicity.[33] Therefore, it is tempting to speculate that the γδ T-cell signalling may be of a lower affinity threshold than cytotoxic $CD8^+$ T cells and will be the focus of future studies.

T cells also displayed highly polycytotoxic profiles in patients infected with influenza viruses *ex vivo* and produced IFN-γ upon co-culture with influenza-infected epithelial cells *in vitro*. Our in-depth dissection of the human TCRγδ repertoires compared key TCRγδ signatures across different ages, tissues and following influenza virus infection. A detailed understanding of human γδ T cells is important as it is increasingly evident that $TCR\gamma\delta^+$ sets in peripheral tissues are distinct from those found in peripheral blood.[34] Defining human γδ T cells according to their paired γδ TCRs, rather than just single γ- or δ-chains, allows us to probe questions concerning the sharing of TCR signatures between individuals, the issue of clonality within individuals and (in the absence of knowing the inducing antigen) questions related to antigen specificity.

Utilising a single-cell multiplex nested RT-PCR to define paired TCR γδ signatures for lymphocytes recovered directly *ex vivo*, we were able to develop a better understanding of how the γδ TCR repertoire may change throughout the course of life. In this analysis, we were not, of course, able to do longitudinal studies within the same individuals, but there are clear patterns associated with the ageing process. The greatest degree of TCR γδ gene segment diversity was found for CB and for spleen samples obtained from donors of different ages. The lack of repeated TCRγδ clonotypes was particularly striking for CB, suggesting that these T cells may be naïve and have not undergone clonal expansion. Previously, from single-cell analyses, the diversity in the CB TCRγδ repertoire was deemed comparable to adults, as these studies were focused of $V\delta2^+$ γδ T cells, and the preferential pairing was shown with $V\gamma9^+$[16] In adults, we found that γδ T-cell TCR diversity was also strongly biased towards the γ9δ2 gene, with fewer alternative γδ gene segment pairings compared to CB and splenic tissues. Clonotypic analysis, however, demonstrated high levels of diversity within adult blood γ9δ2 TCRs, with a minimal number of repeated TCRγδ clonotypes. An intriguing divergence between CB and adult peripheral blood lymphocytes (PBLs) was the prevalence of Jγ*P, a focused CDR3 length of 14 aa and a conserved hydrophobic amino acid at position 97 of the CDR3γ with age. This TCR signature has previously been defined for γδ T-cell recognition of phosphoantigen,[35] supporting the idea that the $V\gamma9^+V\delta2^+$ T cells in the PBL set are clonally expanded by phosphoantigen exposure. Another suggested driver of γδ T cells is butyrophilin gene products of 'self' origin,[36] but the responding T cells do not utilise γ9δ2 and are found mainly in tissue sites. Overall, though, there remains a general deficit in our understanding of what stimulates γδ T cells.

Similar to clonal expansions found for conventional $CD8^+$ TCRαβ T cells in the elderly,[28] large γδ TCR^+ clones were prevalent in older, healthy people, a situation found for T cells that did, or did not, utilise the normally (in younger adults) prominent γ9δ2 TCR pairing. In fact, some older people had few, if any, $\gamma9\delta2TCR^+$ cells within the generally increased (with age) γδ T-cell population, likely reflecting that an individual's history of 'antigen challenge' through life shapes the spectrum γδ T-cell clonal diversity. Such clonal expansions led to a non-normal distribution and distinct CDR3 γδ lengths across different elderly donors. This is the first report of clonal expansions of paired γδ TCRs in elderly adults, with clonal divergence often being associated with differences between the ratio of cell surface expressed TCRγδ and CD3.[25,26]

Our single-cell γδ TCR dissection also demonstrated that the public Vγ9 CDR3γ-CALWEVQELGKKIVF and its variants show evidence of extreme plasticity. Although this public Vγ9 has been described previously,[16] its capacity to pair with ~50 different CDR3δ chains for all donors, ages and sampling sites is a new finding. This finding has potential implications for targeting the public TCRγ in clinical settings perhaps, and as we go forward to analyse disease states, it will be of substantial interest to determine whether the prominence of particular pairing correlates with different infections. However, further studies are

required to understand whether there are any functional differences between each distinct δ pairing with the public Vγ9 TCR.

In human tissues, apart from the γ9δ2 TCR signatures that are prominent for PBLs, we found a much broader range of γδ segments that were unique to CB. In general, the γδ T cells recovered from the lung reflected the γ9δ2 dominance characteristic of the PBLs. Conversely, γδ T cells in across three spleens and one lymph node (LN25) donor consisted of γδ TCR pairs found in CB. However, at the clonal level, γδ TCRs within tissues differed to those within cord or adult blood, in that they were characterised by large clonal expansions. Perhaps these T cells are being driven by local antigen exposure, as suggested by the selective accumulation of $\delta1^+$ for γδ T cells (versus a δ2 PBL signature) obtained by bronchoscopy following airway challenge with tetanus toxoid.[37] Alternatively, this could also reflect selective recruitment.

Our paired chain γδ TCR repertoire analysis further suggests that the prominent $\gamma9\delta2TCR^+$ sets may be directly involved in influenza-mediated immunity. The evidence for this is as follows: (1) the TCR γδ repertoire found for influenza virus-stimulated and cultured IFN-γ-producing γδ T cells displays significantly increased usage of γ9δ2 TCRs (80%); (2) the same TCR γδ clonotypes are found between and within donors following this influenza A virus challenge; (3) the γδ set from CB and an elderly donor who lacked γ9δ2 TCRs did not express any IFN-γ following *in vitro* challenge with influenza-infected epithelial cells.

Collectively, our study provides evidence that γδ T cells and their corresponding TCR γδ repertoires can be shaped by age, localisation and viral exposures. Harnessing γδ T-cell immunity to restrict pathogen growth and promote host recovery and/or tissue healing merits further rigorous analysis as we go forward to analyse disease states and probe possible vaccination and immunotherapy strategies.

METHODS

Human peripheral blood, cord blood and tissues

Buffy packs from healthy donors were obtained from the Red Cross Blood Service (West Melbourne, Australia). Peripheral blood was obtained from healthy adults (age 18–59 years) or elderly donors (age ≥ 60 years), with informed written consent. Umbilical CB was obtained from Mercy Hospital for Women (Heidelberg, Australia). Influenza B virus infection was confirmed in three donors with nasal swabs which were PCR positive for IBV.[38] In donor AH040, two timepoints were available, D7 and D30 post-disease onset. Human tissues (spleens, LNs, lungs) were obtained from deceased organ donors, brain dead (BD) or donation after cardiac death following the family's consent. Spleens and LNs were received from DonateLife Victoria at the time of organ harvest for clinical transplantation. Lung tissues were from the Alfred Hospital's Lung Tissue Biobank. Written informed consent and release of organs for research was obtained with approval from the Australian Blood Cross Blood Service ethics (ID 2015#8). The study was approved by the University of Melbourne Human Ethics Committee (ID 1443389.3 and 1443540), Mercy Health Human Research Ethics Committee (ID R14/25) and the Alfred Hospital (ID #280/14). Experimental work was performed according to the Australian National Health and Medical Research Council Code of Practice. Donor demographics are detailed in Supplementary table 1.

Mononuclear cell isolation

Peripheral blood mononuclear cells were isolated from peripheral blood or CB by density gradient centrifugation over Ficoll-Paque (Amersham Biosciences, Buckinghamshire, UK). Cells were stored in liquid nitrogen (LN2). Tissue samples were maintained in cold PBS and processed within 18 h of organ procurement. Spleen tissues were minced and dissociated into single-cell suspensions by passing through a 70 μm sieve. LNs and lung tissues were minced and subjected to enzymatic digestion in RP-2 media (KDS-RPMI + 2% FCS) containing Collagenase III (1 mg mL^{-1}, Worthington, OH, USA) and DNAse I (0.5 mg mL^{-1}; Roche, Basel, Switzerland). After 1-h digestion at 37°C, enzymatic digestion was inhibited by EDTA (0.01 mM), and digested tissue was passed through sieve and pelleted. Residual red blood cells were lysed with RBC lysis solution (0.168 M ammonium chloride, 0.01 mM EDTA and 12 mM sodium bicarbonate in MilliQ water, Castle hill, NSW, Australia). Cells were subsequently stored in liquid nitrogen.

Purification of human γδ T cells and influenza A virus infection of THP-1 target cells

Sort-purified γδ T cells were maintained at 10^6 cells mL^{-1} in RPMI 1640 medium (10% [vol/vol] heat-inactivated FCS, 2 mM L-glutamine, 10 mM Hepes, 1 mM sodium pyruvate, 100 μM nonessential amino acids and 50 μM 2-ME) containing 10 ng mL^{-1}, IL-15 (PeproTech, Rocky Hill, NJ, USA) for 12–24 h before use for live cell confocal microscopy. Targets cells (THP-1) were infected with influenza A virus at MOI 5 in serum-free RPMI 1640 medium for 1 h at 37°C and 5% CO_2. After incubation, virus-infected THP-1 were washed twice with serum containing RMPI medium to neutralise free-floating viruses. THP-1 were seeded in 1×10^6 mL^{-1} and incubated for 4–6 h at 37°C and 5% CO_2 before proceeding to live cell confocal microscopy.

Chromium release assays

THP-1 cells were infected with H1N1-PR8 influenza A virus at MOI 5 in serum-free RPMI 1640 medium for 1 h at 37°C and 5% CO_2. After incubation, virus-infected THP-1 were washed twice with serum containing RMPI medium to neutralise free-floating viruses. THP-1 were seeded in 1×10^6 mL^{-1} and incubated for 4–6 h at 37°C and 5% CO_2 before proceeding to live cell confocal microscopy. Cytotoxicity was examined by labelling target cells with 100 μCi ^{51}Cr for 90 min at 37°C before washing and adding effector cells serially diluted at various E:T ratios. Co-culture was incubated for 4 h, and then, the percentage of target cell lysis was calculated as [100 × (^{51}Cr release from targets with effectors − ^{51}Cr release from targets alone)/^{51}Cr release from targets with 1% Triton X-100 − ^{51}Cr release from targets alone). The level of ^{51}Cr release from targets alone did not exceed 10% of the total ^{51}Cr release from targets with 1% Triton X-100.

Live cell confocal microscopy

Live cell microscopy was performed as described previously.[19] Suspension target virus-infected and uninfected THP-1 cells were adhered to 8-chamber ibidi chamber slides 15 min before imaging by incubating in serum-free media at 37°C. γδ T cells were labelled with fluo-4 (labelled for 15 min with 1 μM fluo-4 and 0.02% [wt/vol] Pluronic F-127 carrier at 37°C/10% CO_2). Labelled γδ T cells were added to chamber slides seeded with THP-1 in media containing 100 μM PI. Chamber slides were mounted on a heated stage within a temperature-controlled chamber maintained at 37°C and constant CO_2 concentrations (5%) and infused using a gas incubation system with active gas mixer (The Brick; ibidi, Munich, Germany). Optical sections were acquired through the centre of the cells by sequential scans of fluo-4 (excitation 488 nm) and PI (excitation 561 nm) or brightfield/differential interference contrast on a TCS SP5 confocal microscope (Leica, Wetzlar, Germany) using a 40× (NA 0.85) water objective and LAS AF software (Leica). For the 488 and 561 channels, the pinhole was set to 4.2 AU, giving a section thickness of 5 μM and XY pixel size of 378.8 nM. Images were acquired at 6 or 7 frames min^{-1}. Image analysis was performed using LAS AF Lite software (Leica) or Fiji software (Dresden, Germany).

Flow cytometric analyses of γδ T cells

Identification and phenotypic analysis of γδ T cells was performed with the following anti-human monoclonal antibodies (all antibodies were derived from BD biosciences, CA unless indicated): α-CD3-PECF594 or AF700 (clone UCHT1), α-CD4-BV650 (clone OKT4; BioLegend, San Jose, CA, USA), α-CD8-BV605 or PerCPCy5.5 (clone SK1), α-pan TCRγδ- FITC or PeCy7 (clone 2F11, clone B1), α-CD56-PeCy7 (NCAM16.2), α-CD27-AF700 (clone L128), α-CD14-APC-H7 (clone MϕP9), α-CD19-APC-H7 (clone HB19), α-CD45RA-APC (clone L48) and live/dead discrimination marker aqua (Molecular Probes, Eugene, OR, USA). PBMCs were incubated with cell surface monoclonal antibodies for 30 min on ice. For intracellular staining, cells were first surface stained as described above, then washed with MACS buffer (PBS, 0.5% BSA, 2 mM EDTA) fixed and permeabilised using the Cytofix/Cytoperm Plus Fixation/Permeabilization Kit (BD Biosciences, San Jose, CA, USA). Cells were intracellularly stained with α-IFNγ-V450 (clone B2) and α-TNF-AF700 or PE-Cy7 (clone 6401.1111) for 30 min on ice, then washed, and resuspended in MACS buffer. In selected experiments, after surface staining with the Vδ2 (clone B6; Biolegend), cells were fixed and permeabilised with the Transcription Factor Staining Buffer Set according to the manufacturer's instructions (eBioscience, San Diego, CA, USA) and stained intracellularly with monoclonal antibodies for Gzm A (clone CB9, eBioscience), Gzm B (clone GB11), Gzm K (clone GBH69; eBioscience), Gzm M (clone 4B2G4; eBioscience) and perforin (clone B-D48; Biolegend). Samples were acquired on the BD LSR Fortessa with DIVA software version 6 (Ashland, OR, USA). Analyses were performed using FlowJo software version 9.8.3 (Tree Star, Ashland, OR, USA).

In vitro A549 influenza virus infection and PBMC co-culture assay

In vitro infection of the human lung epithelial A549 cells (ATCC, Manassas, VA, USA) was performed as previously described, and schematics of the assay are shown in Figure 3a.[21] Briefly, A549 cells were cultured in RF10 media (RPMI 1640 supplemented with 10% FCS, penicillin, streptomycin, and L-glutamine; Life Technologies, Grand Island, NY, USA, and MEM vitamin solution; Sigma Aldrich, St. Louis, MO, USA). A549 cells at > 95% confluency were infected with A/Puerto Rico/8/1934 H1N1 (PR8) or B/Massachusetts/02/2012 for 1 h at 37°C, 5% CO_2. Following incubation, the A549 monolayer was washed with RF10 and incubated with trypsin versene for 5 min at 37°C. Single-cell suspensions of infected or uninfected A549 cells were then co-cultured with PBMCs (T:E of 1:5) in a 96-well plates for total of 10 h at 37°C, 5% CO_2. Brefeldin A Solution (BFA, BD, San Diego, CA, USA) was added to after 3 h of co-culture. After 10 h of incubation, cells were subjected to intracellular cytokine staining.

PBMC activation by supernatant transfer and monocyte depletion

Supernatant transfers were used to test whether any soluble factors in the IAV-infected A549/PBMC co-culture system could induce anti-viral activity in γδ T cells. Supernatants collected from the virus-infected and uninfected A549/PBMC 10 h co-cultures were transferred to autologous PBMCs and further incubated for 12 h (Figure 3f). In selected experiments, $CD14^+$ monocytes were depleted from PBMC using CD14 magnetic bead (Miltenyi Biotec, Bergisch Gladbach, Germany) prior to A549/PBMC co-culture to assess the role of monocytes in activating γδ T cells during IAV infection.

Paired TCRγδ analyses at the single-cell level of *In vitro* influenza virus-stimulated IFN-γ^+ γδ T cells

Donor PBMCs were stimulated by co-culturing with PR8 (H1N1) influenza virus-infected A549 cells for 6 h without

the addition of protein transport inhibitors. The co-cultured cells were subsequently stained with the IFN-γ Secretion Assay–Detection Kit (PE; Miltenyi Biotec, Auburn, CA, USA), according to the manufacturer's instructions. Cells were stained with additional surface markers, α-CD3, α-pan TCRγδ, α-CD14, α-CD19 and live/dead aqua. Single-cell sorting of IFN-γ-producing or non-producing γδ T cells from A549/PBMC co-cultures was performed, as above (Figure 4a).[23]

Data and statistical analysis

Graphical displays and statistical analyses were performed using Prism GraphPad software, version 7 (La Jolla, CA, USA). Mann–Whitney test was used for comparison between two groups, two-way ANOVA for multiple comparisons, Spearman rank test for correlation, and non-linear regression for CDR3 lengths. Statistical significance described as follows: $*P < 0.05$, $**P < 0.01$ and $***P < 0.001$. Pestle and SPICE software version 1.8 and 5, respectively, was used to analyse co-expression of granzymes and perforin.[39]

ACKNOWLEDGMENTS

We thank ImmunoID facility for FACS sorting and Ms S Gonzalez for technical assistance. The clinical research midwives G Christophers, G Pell, and R Murdoch for sample collection; and the Obstetrics and Midwifery staff of the Mercy Hospital for Women for their co-operation. The Australian National Health and Medical Research Council (NHMRC) NHMRC Program Grant (1071916) to KK supported this work. ML is supported by a Research Fellowship from the Department of Obstetrics and Gynaecology (University of Melbourne) and a Faculty Fellowship from the University of Melbourne. SS was a recipient Victoria India Doctoral Scholarship and Melbourne International Fee Remission Scholarship, University of Melbourne. MK is a recipient of Melbourne International Research Scholarship and Melbourne International Fee Remission Scholarship. MRJ is a NHMRC CDA Research Fellow. KK is a NHMRC Senior Research Level B Fellow (#1102792).

CONFLICT OF INTEREST

The authors declare no conflict of interest.

REFERENCES

1. Macleod AS, Havran WL. Functions of skin-resident γδ T cells. *Cell Mol Life Sci* 2011; **68**: 2399–2408.
2. Sell S, Dietz M, Schneider A *et al.* Control of murine cytomegalovirus infection by γδ T Cells. *PLoS Pathog* 2015; **11**: e1004481.
3. Silva-Santos B, Serre K, Norell H. γδ T cells in cancer. *Nat Rev Immunol* 2015; **15**: 683–691.
4. Morita CT, Beckman EM, Bukowski JF *et al.* Direct presentation of nonpeptide prenyl pyrophosphate antigens to human γδ T cells. *Immunity* 1995; **3**: 495–507.
5. Djaoud Z, Guethlein LA, Horowitz A *et al.* Two alternate strategies for innate immunity to Epstein-Barr virus: one using NK cells and the other NK cells and γδ T cells. *J Exp Med* 2017; **214**: 1827–1841.
6. Neves PC, Rudersdorf RA, Galler R *et al.* $CD8^+$ gamma-delta TCR^+ and $CD4^+$ T cells produce IFN-γ at 5-7 days after yellow fever vaccination in Indian rhesus macaques, before the induction of classical antigen-specific T cell responses. *Vaccine* 2010; **28**: 8183–8188.
7. Dechanet J, Merville P, Lim A *et al.* Implication of γδ T cells in the human immune response to cytomegalovirus. *J Clin Invest* 1999; **103**: 1437–1449.
8. Qin G, Mao H, Zheng J *et al.* Phosphoantigen-expanded human γδ T cells display potent cytotoxicity against monocyte-derived macrophages infected with human and avian influenza viruses. *J Infect Dis* 2009; **200**: 858–865.
9. Qin G, Liu Y, Zheng J *et al.* Type 1 responses of human Vγ9Vδ2 T cells to influenza A viruses. *J Virol* 2011; **85**: 10109–10116.
10. Tu W, Zheng J, Liu Y *et al.* The aminobisphosphonate pamidronate controls influenza pathogenesis by expanding a γδ T cell population in humanized mice. *J Exp Med* 2011; **208**: 1511–1522.
11. Li H, Xiang Z, Feng T *et al.* Human Vγ9Vδ2-T cells efficiently kill influenza virus-infected lung alveolar epithelial cells. *Cell Mol Immunol* 2013; **10**: 159–164.
12. Hayday AC. γδ T cells and the lymphoid stress-surveillance response. *Immunity* 2009; **31**: 184–196.
13. Guo XZ, Dash P, Calverley M *et al.* Rapid cloning, expression, and functional characterization of paired αβ and γδ T-cell receptor chains from single-cell analysis. *Mol Ther Methods Clin Dev* 2016; **3**: 15054.
14. Davey MS, Willcox CR, Joyce SP *et al.* Clonal selection in the human Vδ1 T cell repertoire indicates γδ TCR-dependent adaptive immune surveillance. *Nat Commun* 2017; **8**: 14760.
15. Davey MS, Willcox CR, Hunter S *et al.* The human $V\delta2^+$ T-cell compartment comprises distinct innate-like $V\gamma9^+$ and adaptive $V\gamma9^-$ subsets. *Nat Commun* 2018; **9**: 1760.
16. Ravens S, Schultze-Florey C, Raha S *et al.* Human γδ T cells are quickly reconstituted after stem-cell transplantation and show adaptive clonal expansion in response to viral infection. *Nat Immunol* 2017; **18**: 393–401.
17. Jenkins MR, Rudd-Schmidt JA, Lopez JA *et al.* Failed CTL/NK cell killing and cytokine hypersecretion are directly linked through prolonged synapse time. *J Exp Med* 2015; **212**: 307–317.
18. Lopez JA, Jenkins MR, Rudd-Schmidt JA *et al.* Rapid and unidirectional perforin pore delivery at the cytotoxic immune synapse. *J Immunol* 2013; **191**: 2328–2334.
19. Lopez JA, Susanto O, Jenkins MR *et al.* Perforin forms transient pores on the target cell plasma membrane to facilitate rapid access of granzymes during killer cell attack. *Blood* 2013; **121**: 2659–2668.
20. Ryan PL, Sumaria N, Holland CJ *et al.* Heterogeneous yet stable $V\delta2^+$ T-cell profiles define distinct cytotoxic effector potentials in healthy human individuals. *Proc Natl Acad Sci USA* 2016; **113**: 14378–14383.
21. Loh L, Wang Z, Sant S *et al.* Human mucosal-associated invariant T cells contribute to antiviral influenza immunity via IL-18-dependent activation. *Proc Natl Acad Sci USA* 2016; **113**: 10133–10138.

22. Tsai CY, Liong KH, Gunalan MG *et al.* Type I IFNs and IL-18 regulate the antiviral response of primary human γδ T cells against dendritic cells infected with Dengue virus. *J Immunol* 2015; **194**: 3890–3900.
23. Nguyen TH, Rowntree LC, Pellicci DG *et al.* Recognition of distinct cross-reactive virus-specific $CD8^+$ T cells reveals a unique TCR signature in a clinical setting. *J Immunol* 2014; **192**: 5039–5049.
24. Pauza CD, Cairo C. Evolution and function of the TCR Vgamma9 chain repertoire: it's good to be public. *Cell Immunol* 2015; **296**: 22–30.
25. Paget C, Chow MT, Gherardin NA *et al.* CD3bright signals on γδ T cells identify IL-17A-producing $V\gamma6V\delta1^+$ T cells. *Immunol Cell Biol* 2015; **93**: 198–212.
26. Yokobori N, Schierloh P, Geffner L *et al.* CD3 expression distinguishes two γδT cell receptor subsets with different phenotype and effector function in tuberculous pleurisy. *Clin Exp Immunol* 2009; **157**: 385–394.
27. Gil A, Yassai MB, Naumov YN, Selin LK. Narrowing of human influenza A virus-specific T cell receptor α and β repertoires with increasing age. *J Virol* 2015; **89**: 4102–4116.
28. Kedzierska K, Valkenburg SA, Doherty PC, Davenport MP, Venturi V. Use it or lose it: establishment and persistence of T cell memory. *Front Immunol* 2012; **3**: 357.
29. Dimova T, Brouwer M, Gosselin F *et al.* Effector Vγ9Vδ2 T cells dominate the human fetal γδ T-cell repertoire. *Proc Natl Acad Sci USA* 2015; **112**: E556–E565.
30. Kabelitz D, Wesch D, Pitters E, Zoller M. Characterization of tumor reactivity of human Vγ9Vδ2 γδ T cells *in vitro* and in SCID mice *in vivo*. *J Immunol* 2004; **173**: 6767–6776.
31. Abate G, Spencer CT, Hamzabegovic F *et al.* Mycobacterium-specific γ9δ2 T cells mediate both pathogen-inhibitory and CD40 ligand-dependent antigen presentation effects important for tuberculosis immunity. *Infect Immun* 2016; **84**: 580–589.
32. Anikeeva N, Somersalo K, Sims TN *et al.* Distinct role of lymphocyte function-associated antigen-1 in mediating effective cytolytic activity by cytotoxic T lymphocytes. *Proc Natl Acad Sci USA* 2005; **102**: 6437–6442.
33. Jenkins MR, Tsun A, Stinchcombe JC, Griffiths GM. The strength of T cell receptor signal controls the polarization of cytotoxic machinery to the immunological synapse. *Immunity* 2009; **31**: 621–631.
34. Vantourout P, Hayday A. Six-of-the-best: unique contributions of γδ T cells to immunology. *Nat Rev Immunol* 2013; **13**: 88–100.
35. Adams EJ, Gu S, Luoma AM. Human gamma delta T cells: evolution and ligand recognition. *Cell Immunol* 2015; **296**: 31–40.
36. Di Marco Barros R, Roberts NA, Dart RJ *et al.* Epithelia use butyrophilin-like molecules to shape organ-specific γδ T cell compartments. *Cell* 2016; **167**: 203–218.e217.
37. Wisnewski AV, Cain H, Magoski N, Wang H, Holm CT, Redlich CA. Human γ/δ T-cell lines derived from airway biopsies. *Am J Respir Cell Mol Biol* 2001; **24**: 332–338.
38. Koutsakos M, Illing PT, Nguyen THO *et al.* Human $CD8^+$ T cell cross-reactivity across influenza A, B and C viruses. *Nat Immunol* 2019; **20**: 613–625.
39. Roederer M, Nozzi JL, Nason MC. SPICE: exploration and analysis of post-cytometric complex multivariate datasets. *Cytometry A* 2011; **79**: 167–174.
40. Thomsen MCF, Nielsen M. Seq2Logo: a method for construction and visualization of amino acid binding motifs and sequence profiles including sequence weighting, pseudo counts and two-sided representation of amino acid enrichment and depletion. *Nucleic Acids Res* 2012; **40**: W281–W287.
41. Krzywinski M, Schein J, Birol I *et al.* Circos: an information aesthetic for comparative genomics. *Genome Res* 2009; **19**: 1639–1645.

Supporting Information

Additional supporting information may be found online in the Supporting Information section at the end of the article.